Developmental Cell, Vol. 5, 475–486, September, 2003, Copyright ©2003 by Cell Press

Polar Expression of ErbB-2/HER2 in Epithelia: Bimodal Regulation by Lin-7

Maya Shelly,[1] Yaron Mosesson,[1] Ami Citri,[1] Sara Lavi,[1] Yaara Zwang,[1] Naomi Melamed-Book,[2] Benjamin Aroeti,[2] and Yosef Yarden[1,*]
[1]Department of Biological Regulation
The Weizmann Institute of Science
Rehovot 76100
Israel
[2]Department of Cell and Animal Biology
Institute of Life Sciences
The Hebrew University of Jerusalem
Jerusalem 91904
Israel

Summary

ErbB-2/HER2 drives epithelial malignancies by forming heterodimers with growth factor receptors. The primordial invertebrate receptor is sorted to the basolateral epithelial surface by binding of the PDZ domain of Lin-7 to the receptor's tail. We show that all four human ErbBs are basolaterally expressed, even when the tail motif is absent. Mutagenesis of hLin-7 unveiled a second domain, KID, that binds to the kinase region of ErbBs. The PDZ interaction mediates stabilization of ErbB-2 at the basolateral surface. On the other hand, binding of KID is involved in initial delivery to the basolateral surface, and in its absence, unprocessed ErbB-2 molecules are diverted to the apical surface. Hence, distinct domains of Lin-7 regulate receptor delivery to and maintenance at the basolateral surface of epithelia.

Introduction

The epidermal growth factor (EGF) family of ligands and their receptor tyrosine kinases constitute a signaling module that has been highly conserved throughout evolution. The primordial module found in the nematode *C. elegans* consists of a single EGF-like ligand and one receptor, LET-23 (Aroian et al., 1990). More than ten ligands and four receptors exist in mammals, constituting the ErbB network (reviewed in Yarden and Sliwkowski, 2001). Asymmetric distribution of ErbB and other membrane proteins in epithelial and in neuronal cells is essential for physiological functions (Ikonen and Simons, 1998). Cellular asymmetry depends on the ability to create and maintain distinct subdomains of the plasma membrane, and it involves polarized vesicle trafficking and retention mechanisms (Ikonen and Simons, 1998; Mellman and Warren, 2000).

PDZ domain proteins are vital components of polarized receptor expression (reviewed in Fanning and Anderson, 1999). Most PDZ domains select for a motif containing a hydrophobic carboxy-terminal residue (Songyang et al., 1997). PDZ interactions sort, target, and assemble supramolecular complexes at the cell surface. An example is the role of the PDZ-containing LIN-2/LIN-7/LIN-10 complex in the development of the vulva in *C. elegans* (Kaech et al., 1998). During vulval induction, an EGF-related signal (LIN-3) released by the gonadal anchor cell induces the overlying epithelial precursors to develop the vulva through activation of LET-23 on the basolateral surface of the closest precursor cell. LIN-2, LIN-7, and LIN-10 localize LET-23 to the basolateral surface of precursor cells, and mutations in either of these genes mislocalize LET-23 to the apical surface, thereby inducing a vulva-less phenotype (Kaech et al., 1998; Simske et al., 1996). LIN-2 is a membrane-associated guanylate kinase with a single PDZ domain, whereas LIN-10 contains two PDZ domains and a single phosphotyrosine binding (PTB) domain (Kaech et al., 1998). Likewise, LIN-7 carries a single PDZ domain, and the three proteins form a tripartite complex, in which LIN-2 can bind both LIN-7 and LIN-10, and the PDZ of LIN-7 is free to bind the tail motif of LET-23 (Kaech et al., 1998).

Three forms of Lin-7 exist in vertebrates, and a common amino-terminally located domain, called L27, allows them to bind Lin-2 (Kaech et al., 1998; Straight et al., 2000). Because ErbB-2 is involved in a variety of human epithelial malignancies and it serves as a coreceptor for multiple EGF-like ligands presented primarily to the basolateral surface of epithelial sheets (Yarden and Sliwkowski, 2001), we were interested in its polar distribution. Here, we demonstrate dual binding of ErbB-2 to hLin-7: the degenerate tail motif binds to the PDZ domain of hLin-7, and the kinase domain binds a previously uncharacterized motif of hLin-7. Bivalence of hLin-7 enables bimodal regulation of ErbB-2 polarity in epithelial Madin-Darby canine kidney (MDCK) cells: whereas the PDZ domain maintains ErbB-2 at the basolateral surface, the newly identified short motif of hLin-7 is responsible for delivery of ErbB-2 to the basolateral cell surface.

Results

All Four ErbB Proteins Are Localized to the Basolateral Surface of Epithelial Cells and Bind hLin-7, Irrespective of Their Carboxy-Terminal Motifs

Because binding of the PDZ domain of LIN-7 to a carboxy-terminal motif of LET-23 dictates basolateral localization in vulva precursor cells (Kaech et al., 1998), we addressed the relevance of this mechanism to the four mammalian ErbB proteins. A perfect type I PDZ binding motif is displayed by ErbB-4, whereas ErbB-2 harbors a degenerate motif (Val-Pro-Val), and the termini of ErbB-1 and ErbB-3 contain no consensus motif (Figure 1A). Nevertheless, when ectopically expressed in polarized MDCK epithelial cells, all four human ErbBs exhibited primarily basolateral localization. This was demonstrated either by using domain-specific surface biotinylation (Figure 1B) or by binding of specific radiolabeled

*Correspondence: yosef.yarden@weizmann.ac.il

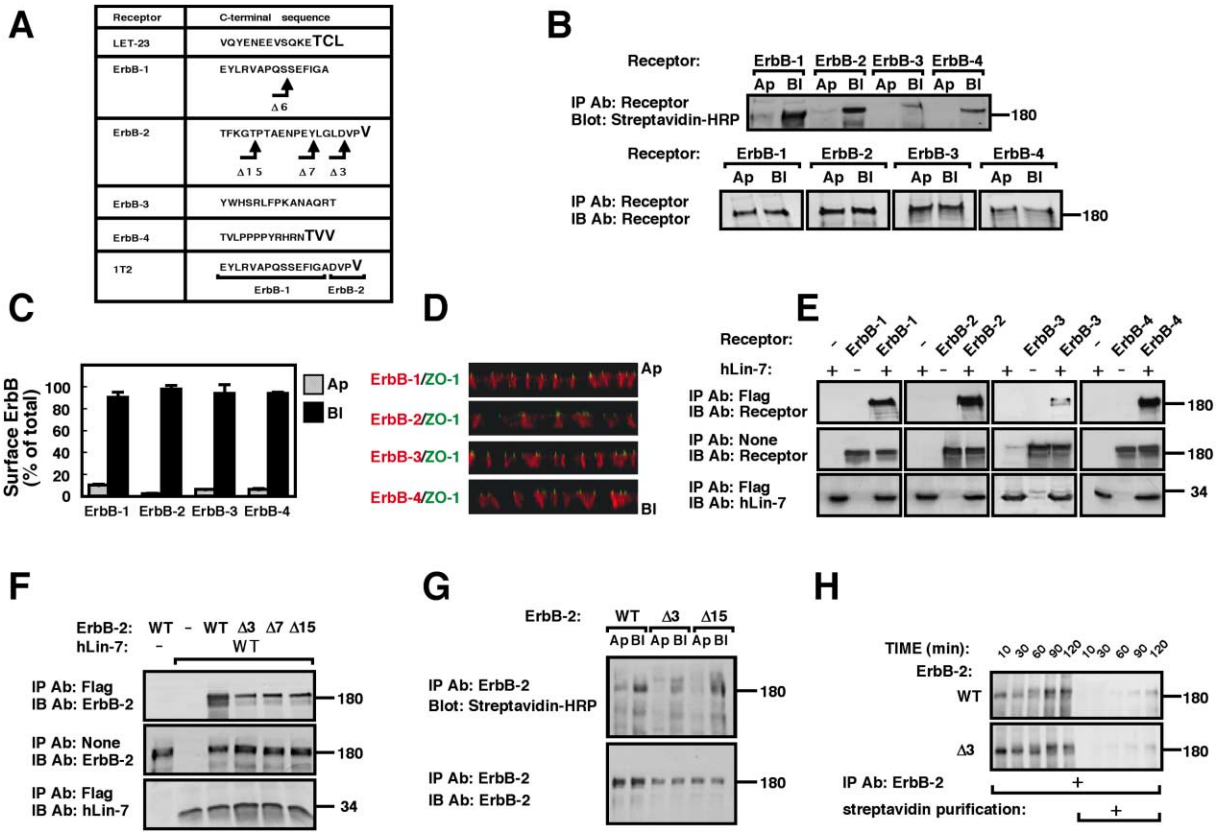

Figure 1. All Four ErbBs Are Localized to the Basolateral Surface of Epithelial Cells, and They Bind hLin-7 Irrespective of Their Tail Motifs

(A) The carboxy-terminal amino acid sequences of the nematode LET-23 and the four human ErbB receptors are shown. Residues conforming to the type I PDZ target motif (T/S-X-I/V/L) are shown in bold. Arrows indicate individual deletion mutants. The fusion receptor 1T2 was constructed by grafting the last four amino acids of ErbB-2 into the tail of ErbB-1.

(B) Filter-grown MDCK cells singly expressing the indicated ErbB protein were labeled on the apical (Ap) or the basolateral (Bl) surface with biotin. Whole-cell extracts were prepared and subjected to immunoprecipitation (IP) and immunoblotting (IB) as indicated.

(C) Filter-grown, ErbB-expressing MDCK cells were incubated with radiolabeled forms of either EGF (ErbB-1), the anti-ErbB-2, L26-mAb (ErbB-2), or NDF (ErbB-3 and ErbB-4). Ligands were added either to the apical (hatched bars) or to the basolateral (black bars) cell surface. Filters were then washed and their radioactivity determined. Nonspecific binding was assayed by using a large excess of the unlabeled ligand. The results are presented as an average and range (bars) of duplicates.

(D) Filter-grown, ErbB-expressing MDCK cells were costained with antibodies to the respective ErbB and a mAb specific to the ZO-1 tight junction protein, followed by fluorescently labeled secondary antibodies (red and green, respectively). Examination was performed using confocal laser scanning microscopy. Reconstructed z plane figures are presented and their apical:basolateral orientation marked.

(E) The four ErbBs were individually expressed in HEK-293T cells, together with a flag-tagged hLin-7. Whole-cell extracts were prepared and analyzed as indicated.

(F) Wild-type (wt) ErbB-2 and the indicated deletion mutants were transiently expressed in HEK-293T cells together with a flag peptide-tagged hLin-7. Anti-flag immunoprecipitates and whole-cell extracts were analyzed with the indicated antibodies.

(G) Filter-grown MDCK cells expressing wild-type (wt) ErbB-2 or the indicated deletion mutants were labeled with biotin on either the apical (Ap) or the basolateral (Bl) surface. Following isolation of ErbB-2, electrophoresis, and electrotransfer, filters were probed with either horseradish peroxidase- (HRP) labeled avidin or with anti-ErbB-2 antibodies.

(H) Filter-grown MDCK cells expressing wt-ErbB-2 or the Δ3 mutant were metabolically pulse labeled for 15 min with ^{35}S-labeled amino acids, chased in fresh medium for increasing time intervals, and subjected to domain-specific biotinylation of the basolateral surface. Radioactive, biotinylated ErbB-2 molecules were isolated by immunoprecipitation and analyzed either directly or following elution and reprecipitation by using streptavidin-agarose.

ligands (Figure 1C). Invariant basolateral targeting of ErbBs was confirmed by the results of immunofluorescence analysis, which used the tight junction marker protein ZO-1 as reference (Figure 1D), and it is in agreement with previous studies that addressed polar distribution of ErbB-1 and ErbB-2 (Borg et al., 2000).

As a first step in elucidating a possible role for Lin-7 in ErbB polarity, we isolated the cDNA of human Lin-7/Veli-1 (Jo et al., 1999). When transiently coexpressed with individual ErbBs, flag-tagged hLin-7 underwent coimmunoprecipitation with all four ErbBs (Figure 1E). Because these results implied that hLin-7 binds ErbBs through a motif distinct from the carboxy-terminal motif, we concentrated on ErbB-2 and constructed three mutants missing three (Δ3), seven (Δ7), or fifteen (Δ15) carboxy-terminal amino acids (see Figure 1A). In line with binding of hLin-7 to the tail motif of ErbB-2, deletion of the carboxy-terminal 3–15 amino acids significantly reduced the extent of interactions with hLin-7 (Figure 1F). Nevertheless, the three deletion mutants of ErbB-2

retained significant binding to hLin-7, and they were targeted to the basolateral surface of MDCK cells (Figure 1G). In summary, the four ErbB proteins are targeted to the basolateral surface of epithelial cells, and they bind hLin-7 in a manner incompletely dependent on the presence of a carboxy-terminal PDZ binding motif.

The PDZ Target Motif of ErbB-2 Is Essential for Stable Retention at but Not for Delivery to the Basolateral Cell Surface

The observed basolateral localization of ErbB proteins may result from targeted delivery or due to a retention mechanism (reviewed in Ikonen and Simons, 1998; Mellman and Warren, 2000). To resolve the mechanism, we compared the fates of wild-type (wt) ErbB-2 and a tail-less mutant (Δ3). First, we pulse labeled ErbB-2 molecules and followed their appearance at the basolateral surface by using domain-specific surface biotinylation and a two-step isolation procedure. These analyses detected neither form of ErbB-2 at the apical surface (data not shown). On the other hand, although both forms complete their processing and reach the basolateral cell surface approximately 90 min after synthesis (Figure 1H), quantification of several delivery assays revealed that 4 hr after their synthesis approximately half wt-ErbB-2 molecules can be recovered from the basolateral surface, but only 15% of the Δ3-ErbB-2 mutants reach the basolateral face.

Consistent with a defect in stability rather than delivery, metabolic labeling revealed that deletion of the PDZ target motif remarkably shortened the half-life of ErbB-2 (Figure 2A). The following lines of evidence indicated that the shorter life span of Δ3 was due to rapid endocytosis and defective recycling. (1) Cells expressing Δ3 internalized a radiolabeled anti-ErbB-2 monoclonal antibody (mAb) at a higher rate than cells expressing wt-ErbB-2 (Figure 2B). (2) Following exposure to a mAb, most (>90%) mutant ErbB-2 molecules were removed from the cell surface within 60 min, but by this time only 40% of wt-ErbB-2 molecules were cleared from the basolateral surface (Figure 2C). (3) Surface biotinylation revealed that the tail-less mutant underwent rapid down-regulation, whereas wt-ErbB-2 displayed relatively long retention at the basolateral surface (Figure 2D). (4) By using an ^{125}I-radiolabeled Fab fragment of an antibody to ErbB-2, we found that wt-ErbB-2 recycles more effectively than a tail-less mutant (Figure 2E). However, inhibition of lysosomal degradation effectively increased recycling of this mutant, while sparing wt-ErbB-2. (5) Unlike surface localization of wt-ErbB-2, Δ3 displayed subapical punctate cytoplasmic localization reminiscent of intracellular vesicles (Figure 2F). Conceivably, the PDZ target motif of ErbB-2 is not involved in biosynthetic delivery to the basolateral surface. Instead, once ErbB-2 reaches the plasma membrane, this motif inhibits receptor internalization and accelerates recycling of internalized molecules back to the basolateral surface.

Bivalent Binding of hLin-7 with ErbB-2

Because our results unveiled relatively weak interactions between hLin-7 and tail-less mutants of ErbB-2 (Figure 1F), the interacting domains were mapped by using transient expression in HEK-293T cells. For reference, we used ErbB-1, whose carboxyl terminus displays no consensus PDZ target motif. Nevertheless, ErbB-1 underwent coimmunoprecipitation with hLin-7, and this interaction was not affected by deletion of carboxy-terminal amino acids (Figure 3A). To identify the interacting portion of hLin-7, we separately expressed the amino-terminal half (mutant denoted ΔP; Figure 3D), or the carboxy-terminal half, including the PDZ domain (ΔN). Because deletion of the amino terminus completely abrogated binding to ErbB-1, and an isolated N terminus retained receptor binding (Figure 3A), the binding site for ErbB-1 must reside in the N-terminal portion of hLin-7. As predicted by the presence of a degenerate PDZ binding motif, wt-ErbB-2 weakly bound to an isolated PDZ domain, whereas Δ3 lost recognition. Nevertheless, Δ3-ErbB-2 retained binding to ΔP-hLin-7 (Figure 3A).

The results we obtained are consistent with bimodal binding of hLin-7 to ErbB-2: whereas the PDZ domain recognizes a carboxy-terminal motif, the amino-terminal portion of hLin-7 recognizes both ErbB-2 and ErbB-1. To test this model, we constructed a chimeric receptor (denoted 1T2; see Figure 1A) comprising full-length ErbB-1 fused to the most carboxy-terminal four amino acids of ErbB-2. As predicted, these four amino acids conferred binding to the isolated PDZ domain (Figure 3A). By utilizing a set of deletion mutants, we concluded that the kinase domain of ErbB-1 binds to the amino-terminal portion of hLin-7 (Figure 3B). This conclusion was extended to ErbB-2 (data not shown) and verified by using the isolated kinase domains of both receptors: when expressed in HEK-293T cells as glutathione-S-transferase (GST) fusion proteins, the kinase region of ErbB-1 (TK1; residues 712–976) and the kinase region of ErbB-2 (TK2-S; amino acids 730–1034, or TK2-L; 730–1075) displayed specific association with the N-terminal part but not with the PDZ domain of hLin-7, and a control protein (GST-CDC37) displayed only background associations (Figure 3C).

Experiments utilizing a series of N-terminal deletion mutants of hLin-7, and both ErbB-1 and Lin-2 as ligands, mapped the ErbB binding site to residues 14–28 (Figure 3D), amino-terminally to the previously defined Lin-2 binding site (L27; Kaech et al., 1998; Straight et al., 2000). Sequence conservation of the kinase-interacting domain (KID) of Veli-1/hLin-7 within the Veli family (see Figure 7A) motivated us to test hVeli-2 and hVeli-3. As shown in Figure 3E, both underwent coimmunoprecipitation with ErbB-1. In addition, the corresponding 21 amino acid-long synthetic peptide inhibited ErbB-1 binding to hLin-7 in a coimmunoprecipitation assay (Figure 3F). As expected, the peptide did not affect Lin-2/Lin-7 interactions. In conclusion, the PDZ and KID domains of hLin-7 enable bivalent binding to target receptors: although both interactions are free of conformational restraints, PDZ binding depends on the identity of the carboxy-terminal receptor's motif, but binding of KID invariably involves the kinase domain.

A Mutant of hLin-7 Arrests Biosynthetic Maturation of ErbB-2

Because our results predicted that hLin-7 binds ErbB proteins either monovalently (ErbB-1 and ErbB-3) or bivalently (ErbB-2 and ErbB-4), the functional consequences of each mode of interaction were addressed. Stable clones of MDCK cells expressing combinations of

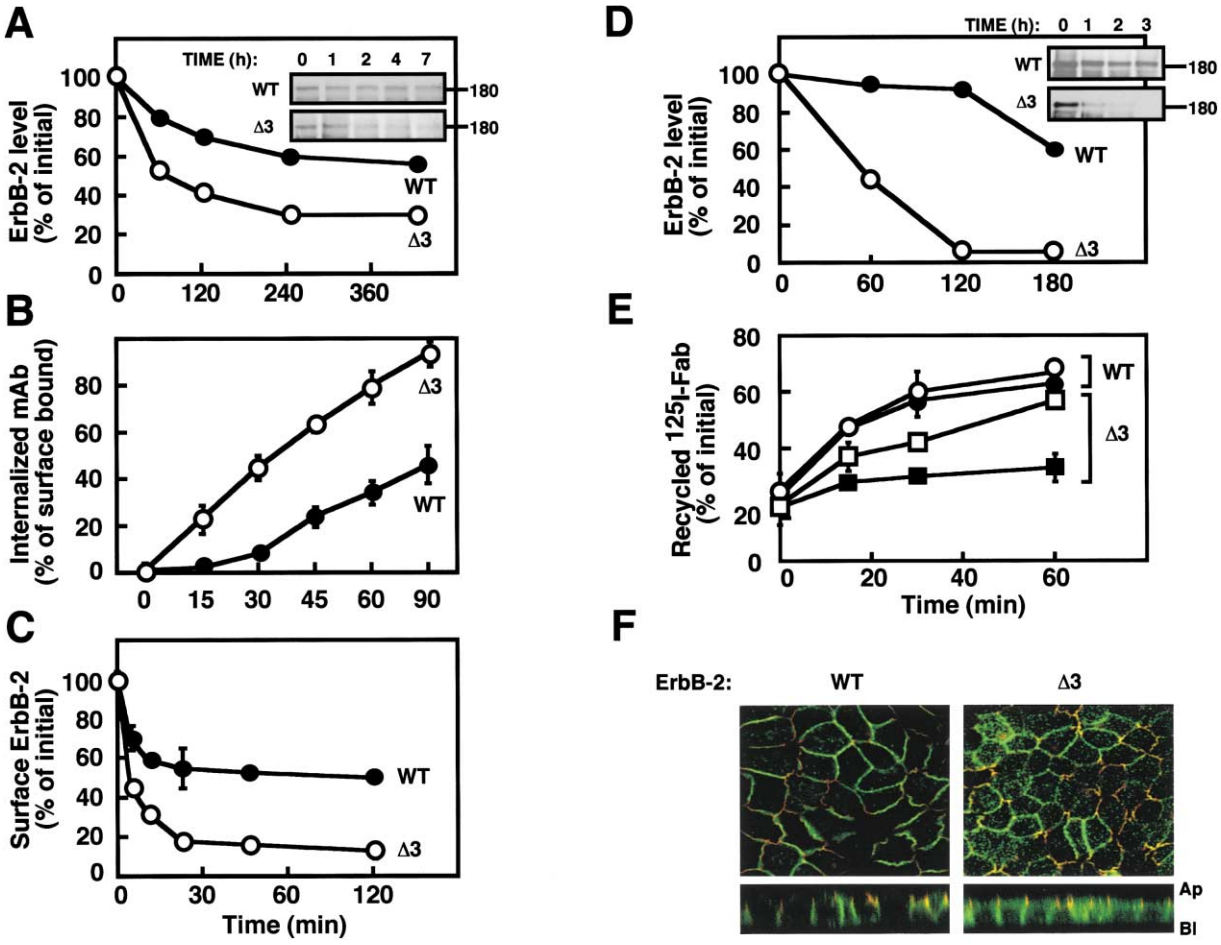

Figure 2. The PDZ Target Motif of ErbB-2 Is Essential for Stable Retention at the Basolateral Cell Surface

Filter-grown MDCK cells expressing ErbB-2 (wt; closed circles) or the Δ3 mutant (open circles) were treated as follows:

(A) Cells were metabolically labeled for 2 hr with [^{35}S]-labeled amino acids, chased in fresh medium, and incubated for the indicated time intervals at 37°C. An autoradiogram of immunoprecpitated ErbB-2 is shown (inset), along with the respective quantification of ErbB-2 signals.

(B) Cells were incubated for 2 hr at 4°C with a radiolabeled L26-mAb that was introduced from the basolateral side. Thereafter, cells were transferred to 37°C for the indicated periods of time. At the end of incubation, cells were treated with a low pH buffer and the fraction of acid-inaccessible (internalized) mAb presented for each time point, relative to the total cell-associated radioactivity prior to transfer to 37°C.

(C) The basolateral surface was exposed to L26-mAb at 37°C, for the indicated time periods. Thereafter, the antibody was removed and the level of surface receptors, relative to the initial number of binding sites, was determined by incubating the cells for 90 min at 4°C with a radiolabeled L26-mAb. The results are expressed as the average fraction (and range; bars) of original binding sites that remained on the cell surface.

(D) Filter-grown cells expressing either wt-ErbB-2 (closed circles) or the Δ3 mutant (open circles) were labeled from the basolateral surface with biotin, incubated for the indicated time intervals at 37°C, and biotinylated ErbB-2 was quantified by immunoprecipitation and blotting with streptavidin-HRP (inset).

(E) Filter-grown MDCK cells expressing wild-type (wt-circles) or Δ3 mutant ErbB-2 (squares) were preincubated for 1 hr at 4°C with radiolabeled Fab-L26 on the basolateral surface, followed by incubation at 37°C for 30 min. Cells were then treated with a low pH buffer and incubated for 1 hr at 4°C with a large excess of unlabeled mAb, followed by incubation at 37°C for the indicated time intervals. Media were then collected and cells treated with a low pH buffer. Surface-bound and internalized Ab fractions were then assayed. The sum of intact radiolabeled Ab (medium and surface bound) was expressed as the percentage of total radioactivity at each time point. The average and range (bars) of duplicate determinations is shown. Sister cultures were similarly treated, except that they were preincubated for 1.5 hr with 0.2 mM chloroquine, which was present throughout the incubation period (open symbols).

(F) Cells were costained with antibodies to ErbB-2 and to the tight junction protein ZO-1, followed by fluorescently labeled secondary antibodies (green and red, respectively). Shown are subapical horizontal (x-y) optical sections at the level of the tight junctions (upper panels) and reconstructed vertical sections (z axis; lower panels).

an ErbB protein (ErbB-1 or ErbB-2) and each monovalent mutant of hLin-7 (ΔN or ΔP) have been established (Figure 4A). Utilizing these clones, we confirmed coimmunoprecipitation of ΔP-hLin-7 with both ErbB-1 and ErbB-2. By contrast, the isolated PDZ domain (ΔN-hLin-7) lost binding to ErbB-1 but retained weak recognition of ErbB-2 (Figure 4B, and data not shown). Unexpectedly, ErbB-2 molecules coprecipitated with ΔN-hLin-7 displayed increased electrophoretic mobility (Figure 4B). Immunofluorescence analysis showed that wt-hLin-7,

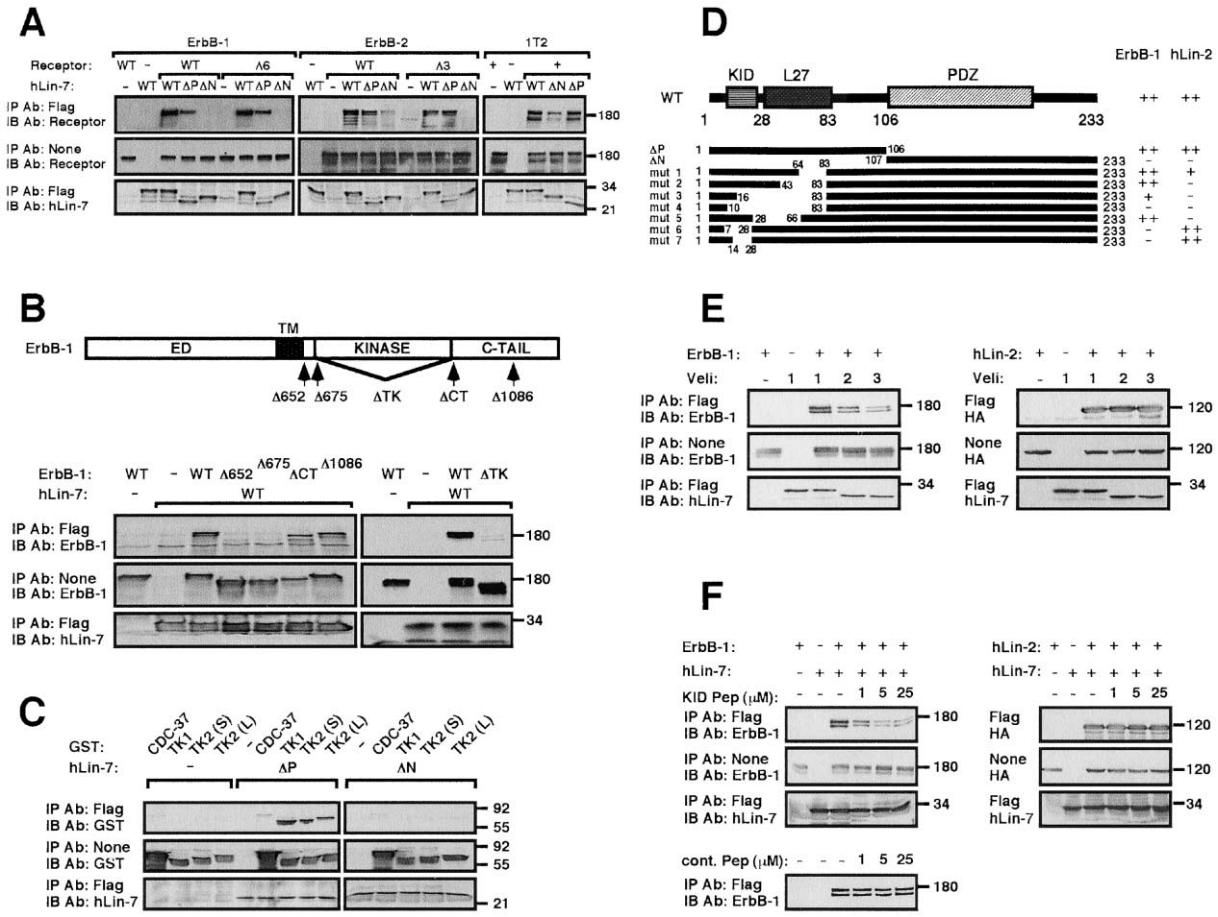

Figure 3. Bimodal Binding of hLin-7 to ErbB-2

(A) The indicated forms of ErbB-1 and ErbB-2 or the 1T2 chimeric receptor were transiently expressed in HEK-293T cells together with a flag-tagged hLin-7 (wild-type [wt], or mutants lacking the N terminus [ΔN] or the PDZ domain [ΔP]). Whole-cell extracts were prepared and analyzed as indicated.

(B) The depicted mutants of ErbB-1 were transiently expressed in HEK-293T cells together with flag-hLin-7. Whole-cell extracts were analyzed, either directly or after immunoprecipitation, with the indicated antibodies.

(C) GST fusion proteins containing the tyrosine kinase domain of either ErbB-1 (denoted TK1) or ErbB-2 (TK2; short [S] and long [L] forms) were transiently expressed in HEK-293T cells, together with the indicated flag-hLin-7 mutants. For control, we used a GST-CDC37 fusion protein. Whole-cell extracts were prepared and analyzed as indicated.

(D) The structure of hLin-7 is schematically depicted. The L27 motif, the PDZ domain, and the newly identified kinase-interacting domain (KID) are shown. The depicted mutants of hLin-7, as well as their relative potency of binding to ErbB-1 and hLin-2, are indicated. Numbers correspond to amino acids.

(E) Flag peptide-tagged isoforms of hLin-7 (Veli-1 through Veli-3) were coexpressed in HEK-293T together with either ErbB-1 or hLin-2 (HA-tagged), and whole-cell lysates were subjected to the indicated analyses.

(F) Coimmunoprecipitation of hLin-7 with either ErbB-1 or hLin-2 was tested in HEK-293T cells. Immunoprecipitation was performed in the presence of increasing concentrations of a synthetic peptide corresponding to the KID motif (residues 7–28 of hLin-7). The experiment was repeated with ErbB-1, hLin-7, and a control synthetic peptide (bottom of left panel).

as well as ΔP-hLin-7, partly colocalized at the basolateral plasma membrane with both ErbB-1 and ErbB-2 (Figures 4C and 4D). In contrast, expression of ΔN-hLin-7 translocated ErbB-2 but not ErbB-1 to a subapical region.

Because disruption of ErbB-2's basolateral localization by a coexpressed ΔN-hLin-7 correlated with the appearance of an altered receptor form (Figure 4B), we hypothesized that deletion of the N terminus mislocalizes hLin-7, and therefore, it arrests maturation of receptors bearing a PDZ target motif. Indeed, PDZ-containing proteins are involved in biosynthetic sorting events of molecules like proTGFα (Fernandez-Larrea et al., 1999). To follow ErbB-2 maturation, we tested the time-dependent acquisition of resistance to endolycosidase H (EndoH), which parallels translocation of EndoH-sensitive high-mannose precursors from the endoplasmic reticulum (ER) to the Golgi apparatus. As reference, we used ErbB-1, whose precursor displayed sensitivity to EndoH in the first hour after synthesis and thereafter gained progressive resistance in a manner independent of ectopic monovalent mutants of hLin-7 (Figure 5A). Although ErbB-2 displayed similar kinetics of maturation, in the presence of ΔN-hLin-7 this receptor remained largely sensitive to EndoH. Consistent with the possibility that the PDZ target motif of ErbB-2 mediates this

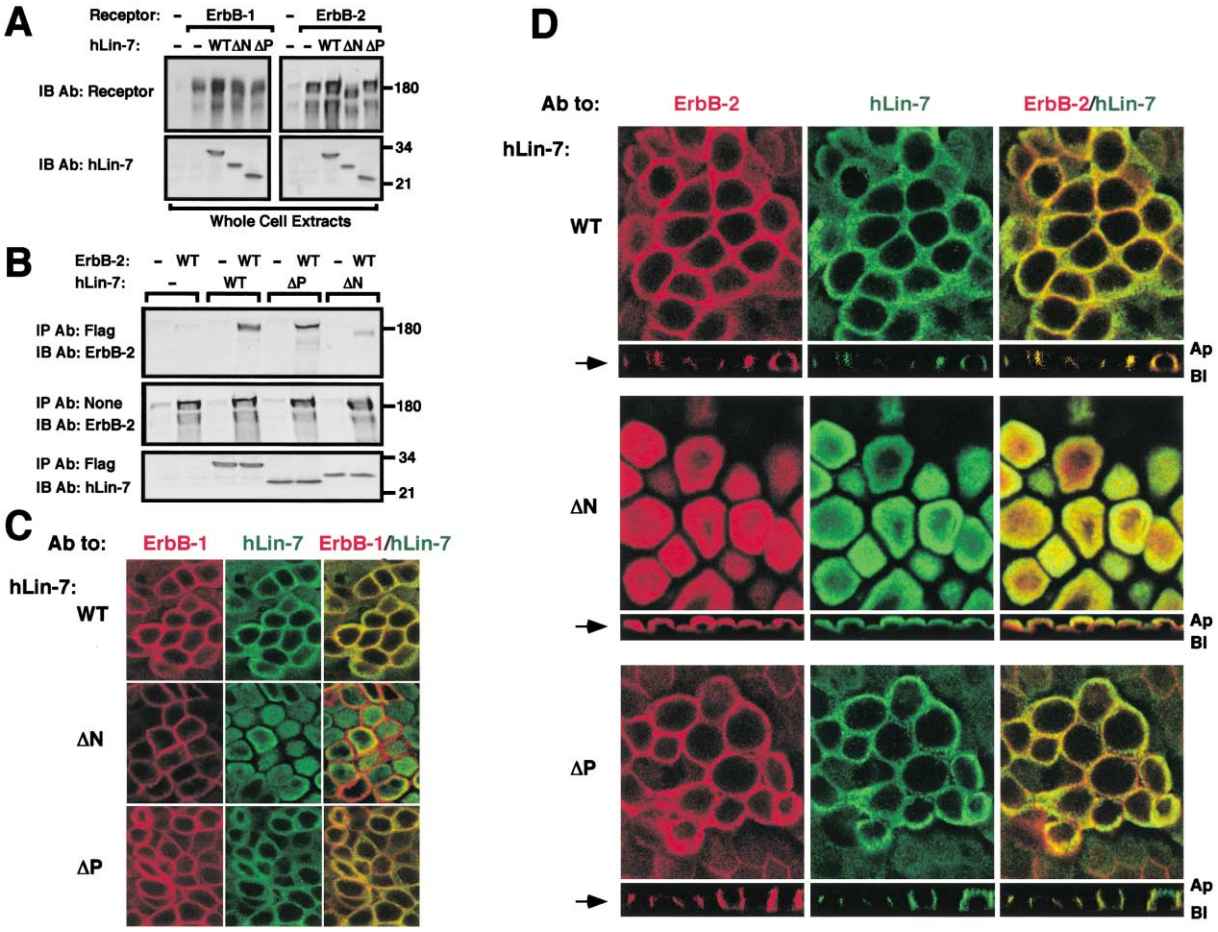

Figure 4. hLin-7 Controls Subcellular Localization of ErbB-2

(A) Whole-cell extracts derived from sublines of MDCK cells stably expressing ErbB-1 or ErbB-2, either alone or in combination with the indicated forms of flag-hLin-7, were analyzed by immunoblotting.

(B) Whole-cell extracts were analyzed as in (A), except that immunoblotting was performed either directly or following immunoprecipitation (IP), as indicated.

(C and D) MDCK cells stably coexpressing ErbB-1 (C) or ErbB-2 (D), together with the indicated forms of hLin-7, were analyzed by immunofluorescence using the indicated antibodies to ErbB (red) and hLin-7 (green). Horizontal and vertical (panel D) optical sections are shown. Arrows indicate the plane of the horizontal sections (panel D). Note the subapical colocalization of ErbB-2 and ΔN-hLin-7 (yellow).

defect, the corresponding deletion mutant of ErbB-2 (Δ3; Figure 5B) gained resistance to EndoH, and grafting the PDZ target motif into the tail of ErbB-1 (1T2 chimeric receptor) conferred sensitivity to EndoH (Figure 5B). Moreover, unlike its parental ErbB-1 molecule, 1T2 colocalized with ΔN-hLin-7 (Figure 5C).

Collectively, these results predicted that hLin-7 binds ErbB molecules soon after their synthesis, a possibility we supported by two lines of evidence. First, biosynthetic labeling indicated that ErbB-2 molecules bind hLin-7 within a few minutes after their biosynthesis in the ER (Figure 5D). Second, when coexpressed with ΔN-hLin-7, ErbB-2 remained colocalized with protein disulfide isomerase (PDI), an ER-resident protein (Figure 5E). In conclusion, by recognizing nascent ErbB molecules in the ER, hLin-7 regulates subsequent receptor sorting to the basolateral surface.

A Monovalent Mutant of hLin-7 Distracts ErbB-2 to the Apical Surface

In view of the possibility that targeting to the basolateral surface is gained while receptors transit from the ER to the trans-Golgi network (TGN; reviewed in Ikonen and Simons, 1998; Mellman and Warren, 2000), the ability of ΔN-hLin-7 to block maturation of ErbB-2 may be informative. Hence, we first addressed the specificity of this effect to the PDZ domain of hLin-7. Because Erbin binds to ErbB-2 through its own PDZ domain (Borg et al., 2000), we tested the ability of the isolated domain to block maturation of ErbB-2. Unlike $PDZ^{Lin\text{-}7}$, when stably expressed in MDCK cells, PDZ^{Erbin} did not affect electrophoretic mobility of a coexpressed ErbB-2 (Figure 5F), consistent with Lin-7 specificity. Next, we analyzed the effect of ΔN-hLin-7 on the polarized distribution of ErbB-2, as well as ErbB-1, a receptor uncoupled to this monovalent mutant. Covalent crosslinking of radiolabeled ligands to MDCK clones coexpressing the respective receptor and ΔN-hLin-7 revealed two effects: along with an overall decrease in surface ErbB-2, the monovalent mutant, unlike the parental hLin-7 or ΔP-hLin-7, significantly increased the fraction of apical ErbB-2 but spared the polarized distribution of ErbB-1 (Figure 6A). Direct binding of a radiolabeled anti-ErbB-2 mAb confirmed comparable levels of apical and basolateral

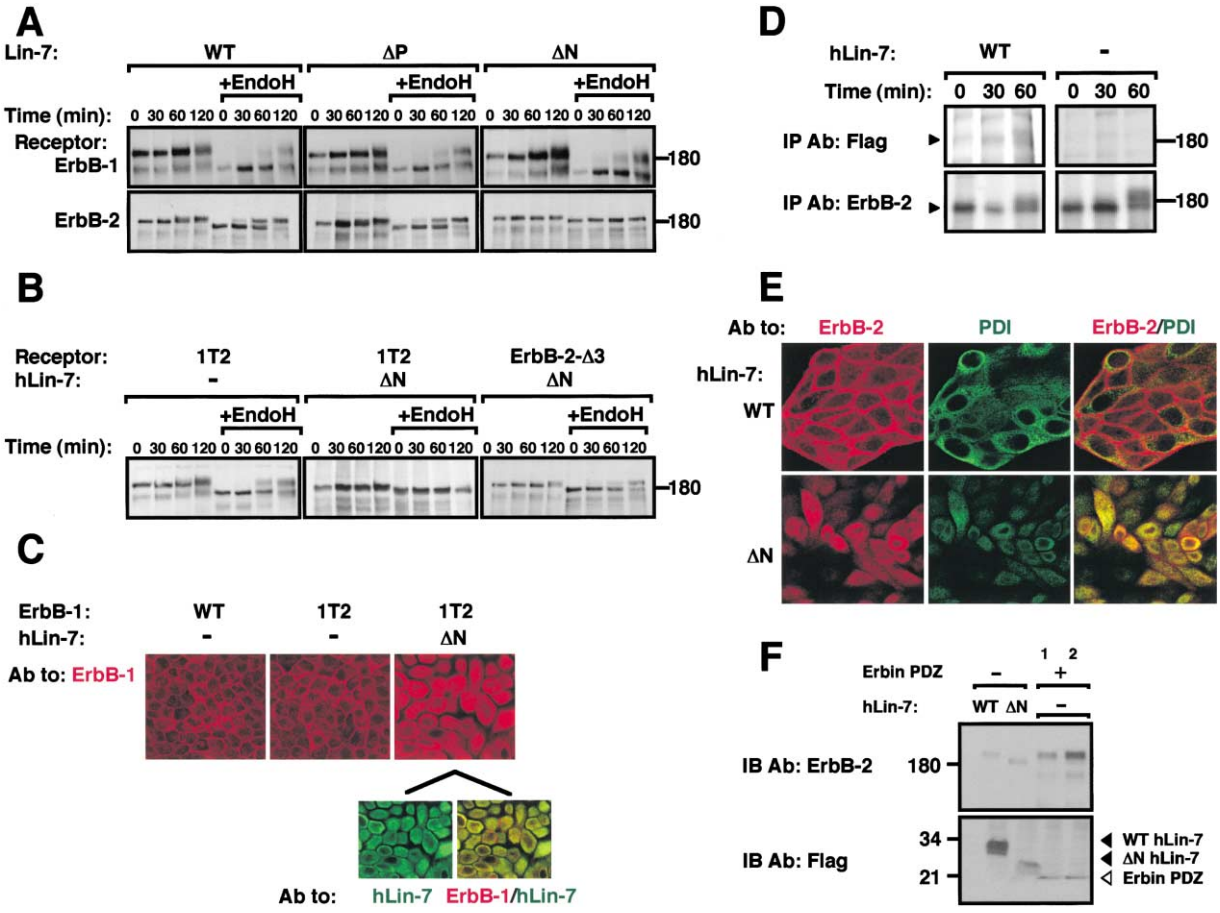

Figure 5. The N-Terminal Portion of hLin-7 Is Necessary for ER-to-Golgi Translocation of ErbB-2

(A and B) Sublines of MDCK cells stably coexpressing the indicated receptors, along with the indicated forms of hLin-7, were metabolically labeled for 15 min with [^{35}S]-methionine, chased in fresh medium, and incubated for the indicated time intervals at 37°C. The immunoprecipitated receptors were untreated or treated with endoglycosidase H (EndoH) prior to gel electrophoresis and autoradiography.

(C) MDCK cells stably expressing ErbB-1 or the 1T2 chimera, either alone or in combination with ΔN-hLin-7, were analyzed by immunofluorescence with antibodies to ErbB-1 (red) and hLin-7 (green). Colocalization is indicated by yellow color (merge panels).

(D) Sublines of MDCK cells stably expressing ErbB-2, either alone or in combination with flag-hLin-7, were metabolically labeled for 15 min as in (A) and incubated for the indicated time intervals at 37°C. Whole-cell extracts were analyzed for coimmunoprecipitation of ErbB-2 (arrowhead) with antibodies to flag-hLin-7.

(E) MDCK cells stably coexpressing ErbB-2 and the indicated forms of hLin-7 were analyzed by immunofluorescence with antibodies to ErbB-2 (red) and the ER marker protein PDI (green). Colocalization is shown in the merge panels (yellow).

(F) Sublines of MDCK cells stably expressing ErbB-2 in combination with a flag-tagged PDZ domain of Erbin were established. Two independently isolated stably transfected clones were extracted and analyzed by immunoblotting as indicated. Sublines of MDCK cells stably expressing ErbB-2 in combination with the indicated forms of hLin-7 were used for control.

ErbB-2 in cells coexpressing ΔN-hLin-7 (Figure 6B), and by using immunofluorescence, we found that a large fraction of ErbB-2 molecules concentrated below the apical surface (Figure 6C). Notably, junctional (ZO-1) and apical (gp135) markers were normally distributed (Figure 6C), as were ErbB-1 and a tail-less mutant of ErbB-2 (Δ3; Figures 6A and 6B), indicating that ΔN-hLin-7 did not obliterate overall cell polarity.

To study the sorting defect induced by ΔN-hLin-7, we biotinylated ErbB-2 molecules at each cell surface. As expected, we observed an unbiased apical:basolateral distribution in cells expressing ΔN-hLin-7, and despite an abnormally broad range of electrophoretic mobilities, only the lighter species of ErbB-2 reached the apical surface (Figure 6D). By contrast, basolaterally expressed molecules displayed normal size. Treatment with EndoH unveiled the basis for dissimilarity: a significant portion of the apically expressed molecules displayed sensitivity to EndoH, whereas basolateral ErbB-2 of ΔN-hLin-7-expressing cells was resistant (Figure 6E). Conceivably, high-mannose pro-ErbB-2 molecules, which are arrested at the ER by ΔN-hLin-7, can leak to the cell surface through two routes: receptors that recruit the endogenous canine Lin-7 transit to the TGN en route to the basolateral surface, but ΔN-hLin-7-bound ErbB-2 molecules shortcut to the apical surface. This model predicts that displacing ΔN-hLin-7 by an ectopically overexpressed full-length hLin-7 will avoid diversion of ErbB-2 to the apical surface and also recover its normal mass. Indeed, graded overexpression of wt-hLin-7 in cells expressing ΔN-hLin-7 increased the fraction of mature ErbB-2 relative to the precursor form

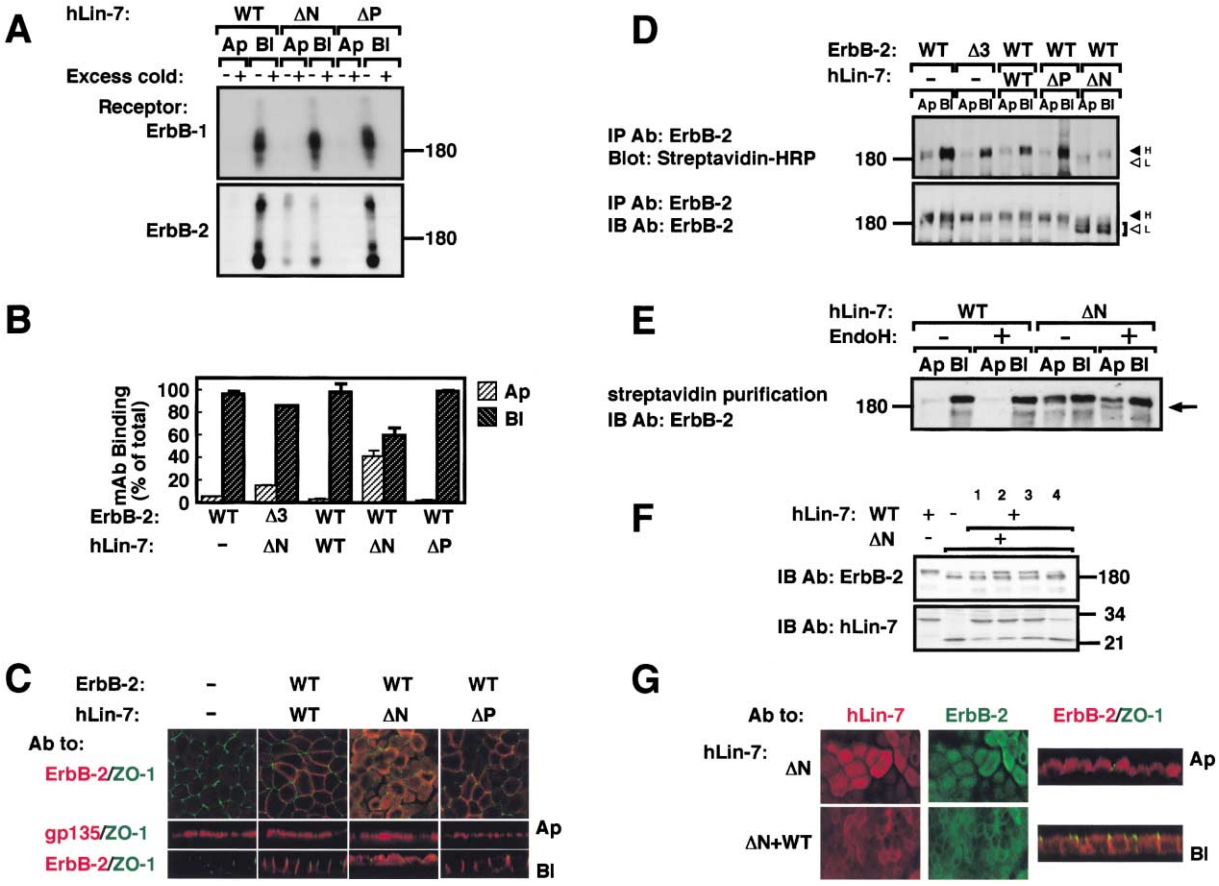

Figure 6. A Monovalent Mutant of hLin-7 Subverts the Immature Form of ErbB-2 to the Apical Surface, but Ectopic wt-hLin-7 Alleviates the Maturation Defect

(A) Filter-grown MDCK cells stably coexpressing ErbB-1 or ErbB-2, along with the indicated forms of hLin-7, were exposed to ^{125}I-EGF (ErbB-1) or to a radiolabeled L26-mAb (ErbB-2). Ligands were added from either the apical (Ap) or the basolateral (Bl) surface, and following incubation, they were covalently crosslinked to their respective receptors by using BS^3. Nonspecific interaction was assayed by using a large excess of the respective unlabeled ligand (*Excess cold*). Shown are autoradiograms of the immunoprecipitated ErbBs.

(B) Filter-grown MDCK cells coexpressing the indicated forms of ErbB-2 and hLin-7 were exposed to a radiolabeled L26-mAb from either the apical (light hatched bars) or the basolateral (dark hatched bars) cell surface. Thereafter, the filters were washed and their radioactivity determined. The results present the average and range (bars) of duplicate determinations of specific antibody binding to each cell surface, relative to total antibody binding to both surfaces.

(C) Filter-grown MDCK cells ectopically expressing ErbB-2 and hLin-7, as indicated, were fixed and stained for ZO-1 (green), ErbB-2 (red), or the apical marker gp135 (red). Both horizontal and vertical optical sections are presented at the level of tight junctions.

(D) The apical (Ap) or the basolateral (Bl) surface of filter-grown MDCK cells coexpressing the indicated forms of ErbB-2 and hLin-7 were biotinylated. Immunoprecipitates of ErbB-2 were probed as indicated. Arrowheads mark high- (H) and low- (L) molecular weight species of ErbB-2, corresponding to the mature and partially processed forms.

(E) Cells were treated as in (D), and biotinylated ErbB-2 was immobilized on streptavidin-agarose. Purified complexes were untreated or treated with endoglycosidase H (EndoH) and analyzed as indicated. Note the appearance of an EndoH-sensitive form of ErbB-2 (arrow) at the apical surface of cells expressing ΔN-hLin-7.

(F) wt-hLin-7 was transfected into MDCK sublines coexpressing ErbB-2 and ΔN-hLin-7. Whole lysates derived from four clones expressing various levels of hLin-7 were analyzed by immunoblotting.

(G) Two sublines of MDCK cells were analyzed: a control clone coexpressing ErbB-2 and ΔN-hLin-7, and a clone that expresses wt-hLin-7 in addition to ErbB-2 and ΔN-hLin-7. Following fixation, cells were stained for hLin-7 (red) and ErbB-2 (green). Alternatively, the merge panels show costaining with antibodies to ErbB-2 (red) and the tight junction protein ZO-1 (green). Horizontal (x-y) and vertical (z plane) optical sections are shown.

(Figure 6F). Moreover, immunofluorescence analyses of ErbB-2 confirmed the ability of an overexpressed wt-hLin-7 to partially repair the sorting defect induced by ΔN-hLin-7 (Figure 6G). This effect was specific to wt-hLin-7 because ErbB-2 displayed abnormal electrophoretic mobility in MDCK cells ectopically coexpressing wt-Erbin and ΔN-hLin-7 (data not shown).

In summary, our results attribute to hLin7 a dual mode of action (see model in Figure 7B): the KID motif invariably binds to the kinase domain of ErbBs. This recognition enables the flanking L27 domain to recruit effectors responsible for ER-to-Golgi translocation and concomitantly sort receptors to the basolateral surface. On the other hand, the PDZ domain may not play a role in

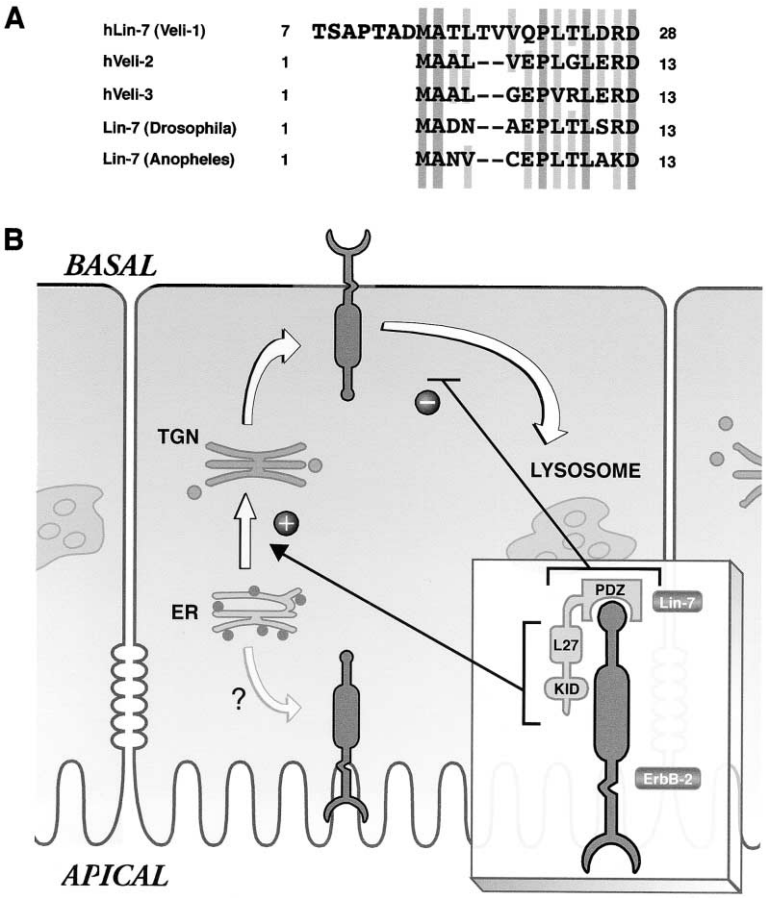

Figure 7. The Dual Mode of ErB-2 Regulation by Lin-7 in Mammalian Epithelia

(A) Alignment of the KID sequence of hLin-7 (residues 7–28) with the corresponding regions of mammalian, *Drosophila*, and *Anopheles* isoforms of LIN-7. Sequence identities are highlighted by dark gray, whereas similarities are indicated by lighter gray color. Residues 7–28 of hLin-7 were used as a synthetic peptide (see Figure 3F).

(B) The dual mode of ErbB-2 regulation by Lin-7 in mammalian epithelia. A typical columnar epithelial sheet is schematically depicted. Normally, the endoplasmic reticulum-(ER) derived ErbB-2 is translocated through the trans-Golgi network (TGN) and reaches primarily the basolateral surface. This process is controlled by binding of the KID region of Lin-7 to the tyrosine kinase (TK) domain of ErbB-2 and recruitment of Lin-2 to the L27 motif (inset figure). Once at the basolateral surface, ErbB-2 is protected from endocytic translocation to the lysosome because its tail motif binds the PDZ domain of Lin-7. How a minor population of ErbB-2 reaches the apical surface remains unsolved.

receptor delivery to the cell surface. Instead, it prevents endocytic delivery of membranal receptors to the lysosome.

Discussion

Two mechanisms contribute to the polarized expression of receptors and channels in epithelial cells: selective targeting and selective stabilization (Ikonen and Simons, 1998; Mellman and Warren, 2000). By concentrating on ErbB-2, we found that one of its tightly associated adaptors, namely Lin-7, combines both mechanisms.

The PDZ Target Motif Inhibits Endocytosis and Enhances Recycling of Basolaterally Expressed ErbB-2 Molecules

Inactivation of the *lin-7* gene (Simske et al., 1996), or preventing binding of LIN-7 to LET-23 by deleting the tail motif of the receptor (Kaech et al., 1998), mislocalized LET-23 and resulted in a vulva-less phenotype. While these lines of evidence identify LIN-7 as a component crucial for basolateral receptor localization in worms, the situation in mammals is complicated by the existence of several other PDZ-containing proteins that bind to the tail of ErbB-2 (Borg et al., 2000; Jaulin-Bastard et al., 2001). Therefore, to approach the issue of ErbB-2 targeting, we deleted the degenerate PDZ target motif and found that the tail-less receptors not only retained basolateral expression, but a significant fraction localized to intracellular vesicles (Figures 1G and 2F). Our results indicate that the vesicular population reflects rapid endocytosis of the truncated receptors from the basolateral surface (Figures 2B and 2C), ineffective recycling, and efficient degradation in lysosomes (Figure 2E). Hence, the PDZ target motif of ErbB-2 may selectively stabilize the receptor at the basolateral surface, rather than actively target the receptor to this surface. Presumably, the PDZ-mediated retention process acts in concert with *cis*-acting signals for basolateral sorting, which often resemble tyrosine- and dileucine-based motifs that specify receptor endocytosis via clathrin-coated pits (Mellman and Warren, 2000). Likewise, a specific clathrin adaptor complex mediates basolateral targeting (Folsch et al., 1999), and cells deficient for the complex mislocalize a large proportion of ErbB-2 to the apical surface (Dillon et al., 2002).

Whether or not hLin-7 is the PDZ-bearing adaptor, which inhibits ErbB-2 internalization in our cellular system, remains unknown. However, it is worth noting that Lin-7 regulates endocytosis and recycling of a chimeric p75 neurotrophin receptor fused to the tail of LET-23 (Straight et al., 2001). In analogy to the proposed inhibitory role of hLin-7, several other PDZ-bearing proteins inhibit internalization of their targets (Hu et al., 2000; Xia et al., 2000). Taken together with lessons learned with other receptors, our results imply that PDZ modules

recruited to the tail of ErbB-2 mobilize retention mechanisms, which inhibit entrapment of the receptor in the clathrin coat and enhance recycling of internalized receptor molecules.

The Kinase-Interacting Domain of hLin-7 Enables Basolateral Sorting at the ER-to-TGN Level

Because ErbB proteins bind with hLin-7 irrespective of the presence of a PDZ target motif, we inferred the existence of a second, PDZ-independent binding site in hLin-7. As expected, the identified site binds a region shared by the four ErbBs, namely the kinase domain (Figure 3). Deletion analyses localized the kinase binding site to a short motif (denoted KID) of hLin-7. This motif is well conserved in evolution, from insects to mammals (Figure 7A). Because KID mutants were unstable, we tested a relatively large deletion mutant lacking the whole N-terminal part of hLin-7. Unlike wt-hLin-7, the ΔN mutant localized to the ER (Figure 5E) and arrested maturation of receptors containing the PDZ target motif (Figures 5A and 5B). Most revealing was the ability of the monovalent mutant to alter the apical:basolateral distribution of ErbB-2 (Figure 6), similar to the effect of ER retention on the distribution of E-cadherin (Chen et al., 1999).

The exit of nascent proteins from the ER depends on *cis*-acting sequences and interactions with sorting proteins (reviewed in Teasdale and Jackson, 1996). For example, the ER-associated PDZ protein syntenin/TACIP18 (Fernandez-Larrea et al., 1999) controls membrane targeting of proTGFα, and PSD-95 similarly regulates the NR1 subunit of NMDA receptors (Standley et al., 2000). The latter masks an ER retention signal in the cytoplasmic domain of NR1. Presumably, the N-terminal part of hLin-7 fulfils a similar role: by folding over the PDZ domain, it may inhibit an intrinsic ER retention signal, whereas the adjacent KID and L27 domains respectively recognize cargoes (e.g., ErbB-2), as well as effectors (e.g., Lin-2) actively regulating basolateral targeting.

A Secretory Pathway that Directly Links the Endoplasmic Reticulum to the Apical Surface?

In the absence of a basolateral signal, proteins are sent to the apical surface by default (Mostov et al., 1992). Alternatively, signals involved in apical sorting of transmembrane proteins rely on glycosyl-phosphatidylinositol anchor modifications, asparagine (N)-linked carbohydrates, or O-glycosylated serine/threonine residues (reviewed in Rodriguez-Boulan and Gonzalez, 1999). Only a relatively small fraction of each ErbB (5%–10%) resides at the apical surface of MDCK cells under steady-state conditions (Figure 1). While this fraction of fully processed molecules may represent basolateral receptors rerouted to the apical face, a different mechanism seems to direct Endo-H-sensitive precursors of ErbB-2 to the apical surface of cells coexpressing ΔN-hLin-7. According to one model, the ER and the plasma membrane form a continuum that allows, for example, phagocytosis of extremely large particles (Gagnon et al., 2002). Thus, when arrested in the ER, nascent ErbB-2 molecules can directly reach the plasma membrane. If correct, this model predicts uncoupling of the basolateral surface from the ER.

Finally, understanding polar distribution of ErbB proteins is relevant to many other receptor tyrosine kinases, and it may shed light on human diseases. Progression of polycystic kidney disease depends on aberrant distribution of ErbB-1, and persistent ErbB signaling predicts poor prognosis of several types of malignancies (reviewed in Yarden and Sliwkowski, 2001). Moreover, mAbs to ErbB-2 and low-molecular weight kinase inhibitors specific to ErbB-1 are already used in the treatment of breast and lung cancer patients, respectively, and both agents modulate receptor trafficking and stability. Future studies will address the possibility that the breakdown of cellular polarity, which frequently accompanies epithelial transformation, can modulate the PDZ-containing tripartite complex in a way that augments tumorigenicity.

Experimental Procedures

Unless indicated, materials were purchased from Sigma (St. Louis, MO), radioactive materials from Amersham Pharmacia Biotech (Buckinghamshire, UK), and antibodies from Santa Cruz Biotechnology (Santa Cruz, CA). Antibodies to hemagglutinin (HA) and flag peptides were from Sigma and Roche (Mannheim, Germany), respectively. IODOGEN and BS^3 were from Pierce (Rochford, IL). Neu differentiation factor (NDF) and monoclonal antibodies to ErbB proteins were generated in our laboratory. An anti-hLin-7 rabbit serum was raised against a bacterial GST-hLin-7 fusion protein. Secondary antibodies used for immunofluorescence were from Jackson ImmunoResearch (West Grove, PA). Fab fragment of mAb-L26 was prepared by papain cleavage and elution through a protein A column.

Construction of Expression Vectors

cDNAs encoding hLin-2, hLin-7, and homologs were isolated from a human keratinocyte library and cloned into pcDNA3 (Invitrogen). The QuickChange mutagenesis kit (Stratagene) was used to introduce point mutations. PCR-based strategies were used to generate hLin-7 mutants, the ΔTK mutant of ErbB-1 (corresponding to amino acids 684–964), and the 1T2 chimera. Inserts encoding for the kinase region of ErbB-1 and ErbB-2 fused to GST were cloned in a modified pEF-BOS vector for expression in mammalian cells. cDNA corresponding to the PDZ domain of Erbin (amino acids 1267–1370) was isolated by RT-PCR.

Generation of Stable MDCK Cell Clones and Transient Transfection to HEK-293T Cells

MDCK cells were transfected by using the calcium phosphate method and selected in medium containing G418 (Life Technologies) and/or hygromycin B (400 μg/ml). At least two independently isolated clones were analyzed. All clones were grown in minimal essential medium (MEM) supplemented with 5% serum. MDCK cells were cultured on Transwell polycarbonate filter inserts (0.4 μm pore size; Costar Corp., Cambridge, MA) at a density of 5×10^5 cells per 12 mm diameter filter. Experiments were conducted 5 days after seeding. HEK-293T cells were transiently transfected using the calcium phosphate method and assayed 48 hr later.

Radioactive Metabolic Labeling

Filter-grown cells were rinsed twice and preincubated for 2 hr in cysteine- and methionine-free medium supplemented with 10% dialyzed serum. Thereafter, cells were labeled for 15 min or 2 hr with a mixture of ^{35}S-labeled amino acids. The labeling medium was then replaced with a fresh medium supplemented with nonradioactive amino acids. Following incubation, cell rinsing, and lysis, extracts were cleared and analyzed.

Immunofluorescence and Cell Surface Biotinylation

Previously described fixation protocols were used for immunofluorescence (Orzech et al., 2001). A combination of Bio-Rad MRC-1024 confocal instrument and a Zeiss Axiovert 135M inverted microscope was used to acquire images. For biotinylation, filter-grown cells

were washed three times with ice-cold phosphate-buffered saline (PBS) and then incubated for 60 min at 4°C with N-hydroxysuccinimide-biotin (biotin-X-NHS, 0.5 mg/ml; Calbiochem) dissolved in borate buffer (10 mM boric acid, 150 mM NaCl [pH 8.0]). Coupling of biotin was blocked by cell rinsing with a solution of 15 mM glycine in PBS.

Radio-Ligand Binding and Covalent Crosslinking Assays

Growth factors were labeled by using IODOGEN and antibodies by using the chloramine-T method. For binding assays, filter-grown cells were washed twice with binding buffer (MEM supplemented with 0.5% bovine serum albumin and 20 mM HEPES [pH 7.5]) and then incubated for 2 hr at 4°C with a radiolabeled ligand added to either the apical or to the basolateral surface. The cells were washed three times with ice-cold binding buffer and their radioactivity determined. Nonspecific binding was calculated by performing the binding assays in the presence of a 100-fold excess of the corresponding unlabeled ligand. For covalent crosslinking, cells were incubated on ice for 1.5 hr with either ^{125}I-EGF (10 ng/ml) or a radiolabeled mAb (L26; 50 ng/ml, 10^5 cpm/ml) added to the apical or to the basolateral cell surface. Thereafter, cells were washed with PBS and incubated for 20 min at room temperature with BS^3 (1 mM). Following quenching in glycine- (15 mM) containing PBS, cells were extracted and analyzed.

Antibody Internalization, Receptor Downregulation, and Antibody Recycling Assays

Filter-grown cells were incubated for 2 hr at 4°C with ^{125}I-labeled mAb (10^5 cpm/ml) added to the basolateral surface. The cells were then transferred to 37°C and incubated for various intervals. Thereafter, cells were put on ice, and the cellular distribution of the radiolabeled antibody was determined by using a 5 min long incubation with a stripping solution (150 mM acetic acid [pH 2.7], containing 150 mM NaCl). To follow ErbB-2 downregulation, filter-grown cells were washed and incubated at 37°C for various time intervals without or with mAbs (20 μg/ml). Following washing, surface-bound mAbs were removed by using stripping solution, and the number of surface ErbB-2 was determined by incubating cells for 90 min at 4°C with a radiolabeled mAb. To follow receptor recycling, we used a previously described protocol (Kornilova et al., 1996) and a ^{125}I-Fab fragment of L26 mAb.

Endoglycosidase Digestion and Receptor Delivery Assay

Receptor immunoprecipitates were washed in HNTG solution (20 mM HEPES [pH 7.5], 150 mM NaCl, 0.1% Triton X-100, and 10% glycerol), resuspended in 50 mM Na-citrate buffer (pH 5.7), and incubated for an hour at 37°C with endoglycosidase H (10 units) in a total volume of 40 μl. To follow receptor delivery, cells were pulse labeled for 15 min at 37°C, washed, and then chased for various intervals at 37°C. Thereafter, surface proteins were biotinylated on either the apical or the basolateral surface, followed by quenching with PBS-glycine. Cells were then extracted and ErbB-2 immunoprecipitated. The washed immunobeads were boiled for 5 min in 1% sodium-dodecylsulfate (SDS; 20 μl), and biotinylated ErbB-2 was precipitated by using streptavidin-agarose.

Acknowledgments

We thank Drs. Borg and Birnboim for plasmids; Dr. Ena Orzech for advice; and the microscopy unit of the Hebrew University for immunofluorescence. This work was supported in part by grants from the National Cancer Institute (grant CA72981), the European Community (grant QLG1-2000-02160), the United States-Israel Binational Science Foundation (grant 1999-277), and the Israel Science Foundation funded by the Israel Academy of Sciences.

Received: January 14, 2003
Revised: June 3, 2003
Accepted: July 9, 2003
Published: September 8, 2003

References

Aroian, R.V., Koga, M., Mendel, J.E., Ohshima, Y., and Sternberg, P.W. (1990). The let-23 gene necessary for Caenorhabditis elegans vulval induction encodes a tyrosine kinase of the EGF receptor subfamily. Nature *348*, 693–699.

Borg, J.P., Marchetto, S., Le Bivic, A., Ollendorff, V., Jaulin-Bastard, F., Saito, H., Fournier, E., Adelaide, J., Margolis, B., and Birnbaum, D. (2000). ERBIN: a basolateral PDZ protein that interacts with the mammalian ERBB2/HER2 receptor. Nat. Cell Biol. *2*, 407–414.

Chen, Y.T., Stewart, D.B., and Nelson, W.J. (1999). Coupling assembly of the E-cadherin/beta-catenin complex to efficient endoplasmic reticulum exit and basal-lateral membrane targeting of E-cadherin in polarized MDCK cells. J. Cell Biol. *144*, 687–699.

Dillon, C., Creer, A., Kerr, K., Kumin, A., and Dickson, C. (2002). Basolateral targeting of ERBB2 is dependent on a novel bipartite juxtamembrane sorting signal but independent of the C-terminal ERBIN-binding domain. Mol. Cell. Biol. *22*, 6553–6563.

Fanning, A.S., and Anderson, J.M. (1999). Protein modules as organizers of membrane structure. Curr. Opin. Cell Biol. *11*, 432–439.

Fernandez-Larrea, J., Merlos-Suarez, A., Urena, J.M., Baselga, J., and Arribas, J. (1999). A role for a PDZ protein in the early secretory pathway for the targeting of proTGF-alpha to the cell surface. Mol. Cell *3*, 423–433.

Folsch, H., Ohno, H., Bonifacino, J.S., and Mellman, I. (1999). A novel clathrin adaptor complex mediates basolateral targeting in polarized epithelial cells. Cell *99*, 189–198.

Gagnon, E., Duclos, S., Rondeau, C., Chevet, E., Cameron, P.H., Steele-Mortimer, O., Paiement, J., Bergeron, J.J., and Desjardins, M. (2002). Endoplasmic reticulum-mediated phagocytosis is a mechanism of entry into macrophages. Cell *110*, 119–131.

Hu, L.A., Tang, Y., Miller, W.E., Cong, M., Lau, A.G., Lefkowitz, R.J., and Hall, R.A. (2000). beta 1-adrenergic receptor association with PSD-95. Inhibition of receptor internalization and facilitation of beta 1-adrenergic receptor interaction with N-methyl-D-aspartate receptors. J. Biol. Chem. *275*, 38659–38666.

Ikonen, E., and Simons, K. (1998). Protein and lipid sorting from the trans-Golgi network to the plasma membrane in polarized cells. Semin. Cell Dev. Biol. *9*, 503–509.

Jaulin-Bastard, F., Saito, H., Le Bivic, A., Ollendorff, V., Marchetto, S., Birnbaum, D., and Borg, J.P. (2001). The ERBB2/HER2 receptor differentially interacts with ERBIN and PICK1 PSD-95/DLG/ZO-1 domain proteins. J. Biol. Chem. *276*, 15256–15263.

Jo, K., Derin, R., Li, M., and Bredt, D.S. (1999). Characterization of MALS/Velis-1, -2, and -3: a family of mammalian LIN-7 homologs enriched at brain synapses in association with the postsynaptic density-95/NMDA receptor postsynaptic complex. J. Neurosci. *19*, 4189–4199.

Kaech, S.M., Whitfield, C.W., and Kim, S.K. (1998). The LIN-2/LIN-7/LIN-10 complex mediates basolateral membrane localization of the *C. elegans* EGF receptor LET-23 in vulval epithelial cells. Cell *94*, 761–771.

Kornilova, E., Sorkina, T., Beguinot, L., and Sorkin, A. (1996). Lysosomal targeting of epidermal growth factor receptors via a kinase-dependent pathway is mediated by the receptor carboxyl-terminal residues 1022–1123. J. Biol. Chem. *271*, 30340–30346.

Mellman, I., and Warren, G. (2000). The road taken: past and future foundations of membrane traffic. Cell *100*, 99–112.

Mostov, K., Apodaca, G., Aroeti, B., and Okamoto, C. (1992). Plasma membrane protein sorting in polarized epithelial cells. J. Cell Biol. *116*, 577–583.

Orzech, E., Livshits, L., Leyt, J., Okhrimenko, H., Reich, V., Cohen, S., Weiss, A., Melamed-Book, N., Lebendiker, M., Altschuler, Y., et al. Interactions between adaptor protein-1 of the clathrin coat and microtubules via type 1a microtubule-associated proteins. J. Biol. Chem. *276*, 31340–31348.

Rodriguez-Boulan, E., and Gonzalez, A. (1999). Glycans in post-Golgi apical targeting: sorting signals or structural props? Trends Cell Biol. *9*, 291–294.

Simske, J.S., Kaech, S.M., Harp, S.A., and Kim, S.K. (1996). LET-23 receptor localization by the cell junction protein LIN-7 during *C. elegans* vulval induction. Cell *85*, 195–204.

Songyang, Z., Fanning, A.S., Fu, C., Xu, J., Marfatia, S.M., Chishti, A.H., Crompton, A., Chan, A.C., Anderson, J.M., and Cantley, L.C. (1997). Recognition of unique carboxyl-terminal motifs by distinct PDZ domains. Science *275*, 73–77.

Standley, S., Roche, K.W., McCallum, J., Sans, N., and Wenthold, R.J. (2000). PDZ domain suppression of an ER retention signal in NMDA receptor NR1 splice variants. Neuron *28*, 887–898.

Straight, S.W., Karnak, D., Borg, J.P., Kamberov, E., Dare, H., Margolis, B., and Wade, J.B. (2000). mLin-7 is localized to the basolateral surface of renal epithelia via its NH(2) terminus. Am. J. Physiol. Renal Physiol. *278*, F464–F475.

Straight, S.W., Chen, L., Karnak, D., and Margolis, B. (2001). Interaction with mLin-7 alters the targeting of endocytosed transmembrane proteins in mammalian epithelial cells. Mol. Biol. Cell *12*, 1329–1340.

Teasdale, R.D., and Jackson, M.R. (1996). Signal-mediated sorting of membrane proteins between the endoplasmic reticulum and the golgi apparatus. Annu. Rev. Cell Dev. Biol. *12*, 27–54.

Xia, J., Chung, H.J., Wihler, C., Huganir, R.L., and Linden, D.J. (2000). Cerebellar long-term depression requires PKC-regulated interactions between GluR2/3 and PDZ domain-containing proteins. Neuron *28*, 499–510.

Yarden, Y., and Sliwkowski, M.X. (2001). Untangling the ErbB signalling network. Nat. Rev. Mol. Cell Biol. *2*, 127–137.